Published in final edited form as:
Adv Funct Mater. 2012 July 24; 22(14): 3023–3028. doi:10.1002/adfm.201200004.

Polyglycerol-Dendronized Perylenediimides as Stable, Water-Soluble Fluorophores

Dr. Si Kyung Yang and **Prof. Steven C. Zimmerman**
Department of Chemistry, University of Illinois at Urbana-Champaign, Urbana, Illinois 61801 (USA)

Steven C. Zimmerman: sczimmer@illinois.edu

Abstract

The synthesis and photophysical properties of water-soluble, fluorescent polyglycerol-dendronized perylenediimides **1**–**4** are reported. The polyglycerol dendrons, which are known to be highly biocompatible, are found to confer high water-solubility on the perylenediimide in aqueous media while retaining its excellent fluorescent properties. Furthermore, intramolecular cross-linking of the polyglycerol dendrons using the ring-closing metathesis reaction not only enhances the photostability but also reduces the size of perylenediimide-cored dendrimers. The permeability of the various dendritic shells is probed using heavy metal ion quenchers and compared to non-dendritic but water-soluble perylenediimide **5**.

Keywords

perylenediimide; polyglycerol; dendrimer; cross-linking; photostability

1. Introduction

Fluorescence microscopy is a powerful tool for the visualization of biological processes in living cells, including protein localization, DNA replication, enzyme catalysis, gene regulation, and cellular metabolism.[1] These biological studies require highly bright, water-soluble, biocompatible, and photostable fluorophores that absorb and emit above 500 nm to reduce the auto-fluorescence background of cells.[2] Although many organic dyes such as fluorescein, rhodamine, cyanine, and BODIPY are commercially available and have been widely used for fluorescence microscopy,[3] arguably no existing fluorophore fulfills all the above requirements. In particular, nearly all fluorophores suffer from photobleaching, which often limits the long-term visualization of *in vivo* cellular events.

In this regard, perylenediimides (PDIs) have attracted considerable attention because of their exceptional thermal and photochemical stability with high fluorescence quantum yields in organic solvents.[4] Although the extensive use of PDIs as industrial pigments depends upon their low solubility, it was the development of soluble and functional PDIs that led to their broader use in areas that range from dye lasers to solar cells and photovoltaic devices.[5] Despite these advances, a major challenge to the use of PDIs in bioapplications, remains making them water-soluble and nonaggregating in aqueous media while retaining their exceptional fluorescent properties. Müllen and co-workers reported the preparation of highly water-soluble and fluorescent PDIs by incorporating ionic moieties such as sulfonate, pyridinium, and quaternary ammonium groups into the bay regions.[6] Another strategy,

Correspondence to: Steven C. Zimmerman, sczimmer@illinois.edu.

introduced by Haag and co-workers, is based on the attachment of water-soluble polyglycerol dendrons (PGDs) at the imide positions.[7] The bay-substituted PDIs have the added advantages of a significant red shift in the absorption maximum with a larger Stokes shift and easy incorporation of a single reactive group,[8] whereas the latter allows for the nonionic character of PDIs, potentially minimizing undesired association with membranes and other charged biomolecules.

By combining the advantages of the two approaches, we recently reported clickable, monofunctional, uncharged, water-soluble PGD-PDIs that can be singly linked to biomolecules, and their applications in single-molecule studies and target-specific biolabeling.[9] The key finding was the ability of uncharged PGD-PDIs to specifically label proteins on the surface of living bacteria cells, which was not possible with water-soluble, ionic PDI analogues. With the importance of the dendronized, neutral character of PDIs established in our initial study, we have further investigated their utility through a structure-property relationship. In particular, we report herein a comparison of the following PDI derivatives: (i) charged, nondendronized PDIs, (ii) neutral, uncross-linked PGD-PDIs, and (iii) intramolecularly cross-linked PGD-PDIs.

In this study the design involves encapsulating a water-insoluble PDI within a protective polyglycerol dendritic shell to produce highly fluorescent and water-soluble PGD-PDIs. The synthetic approach also allows the allyl end-groups of the PGD-PDIs to be cross-linked by the ring-closing metathesis (RCM) reaction.[10] The RCM-based cross-linking provides additional photostability as well as significant size reduction of PGD-PDIs that might be unnecessarily large for some applications. Various heavy metal ions can quench the fluorescence of the PDI and were used as probes of the permeability of the dendritic shell.

2. Results and Discussion

The structures of PGD-PDIs used in this study feature fluorescent PDI cores encapsulated within four (**1**) and eight (**2**) polyglycerol dendrons (Fig. 1). In addition to their ease of synthesis and high water-solubility,[11] the polyglycerol dendrimers were appealing because of their high biocompatibility[12] and availability of a range of core-functionality.[13] Ultimately, the even greater accessibility of hyperbranched polyglycerols,[14] including those that are core-functionalized,[15] increased the appeal of this approach.

The synthesis of PGD-PDIs **1**–**4** is outlined in Scheme 1. Dendritic PDIs **1** and **2** were both prepared by the dihydroxylation of the allyl ether end-groups in **6** and **7**, respectively. The key intermediates, PGD-PDIs **6** and **7** containing 32 and 64 allyl end-groups, respectively, were synthesized by HATU-mediated amide coupling between PDI cores with four (for **6**) and eight (for **7**) carboxylic acids and amine-functionalized PGDs. Both **6** and **7** were purified by column chromatography and size-exclusion chromatography (SEC), and the purity was determined by ^{1}H NMR spectroscopy and analytical SEC, as well as MALDI-TOF mass spectrometry, which confirmed the complete attachment of four dendrons for **6** and a mixture of seven and eight attachments for **7**, with the latter predominating (Fig. 2). The polyallylated **6** and **7** were then dihydroxylated using 2 mol% of $K_2OsO_4{\cdot}2H_2O$ per alkene to obtain PGD-PDIs **1** and **2** with 64 and 128 peripheral hydroxyl groups, respectively. The use of $K_2OsO_4{\cdot}2H_2O$ was preferred because of its lower volatility than osmium tetraoxide. The full conversion of **6** and **7** to **1** and **2**, respectively, was confirmed by the complete disappearance of resonances corresponding to alkene protons at δ 5.8 and δ 5.4–5.0 ppm in the ^{1}H NMR spectra, and by complete shifts of molecular ion peaks from 4630.4 and 8149.4 to 5715.7 and 10344.0 *m*/*z* for **1** and **2**, respectively, in the MALDI-TOF mass spectra (Fig. 2).

The availability of **6** and **7**, made it possible to cross-link their surfaces using the RCM reaction thereby producing analogues **3** and **4**, respectively (Fig. 1).[16] It has been shown that long-range surface cross-links are favored[17a] and that the cross-linked dendrimers are significantly smaller and denser after the RCM surface treatment.[17] This type of "shrink-wrapping" may increase the degree of encapsulation by making a tighter and denser dendritic shell. The efficient intramolecular cross-linking can be achieved using a catalytic amount of Grubbs-type catalyst under high dilution conditions. Thus, **6** and **7** were cross-linked in dichloromethane (37 μM for **6** and 12 μM for **7**) using the RCM reaction with 4 mol% of Grubbs' second-generation catalyst[18] per alkene to give the cross-linked PGD-PDIs **8** and **9**, respectively.

The cross-linking process was monitored by a combination of ^{1}H NMR and MALDI-TOF mass spectra, and SEC. The ^{1}H NMR spectra showed a significant broadening of all signals, nearly complete loss of the resonance corresponding to the terminal alkene protons (-CH=CH_2) at δ 5.4–5.0 ppm, and new internal alkene signals (-C*H*=C*H*-) appearing at δ 6.0-5.4 ppm. Based on these NMR data we estimate >90–95% cross-linking. Upon complete cross-linking, the RCM reactions are expected to result in the mass reductions of 448.5 Da for **8** and 897.0 Da for **9** corresponding to the loss of 16 and 32 ethylene groups, respectively. The MALDI mass spectra of **8** and **9** showed the most intense peak at 4179.1 (for 16 cross-links) and 7251.6 *m*/*z* (for 32 cross-links), respectively, corresponding to fully cross-linked dendrimers in each case (Fig. 2). The peak for **9**, however, was broad indicating a range of masses as a result of incomplete cross-linking. The extent of size contraction with cross-linking was monitored by comparing the SEC traces of PGD-PDIs **6**–**9** (Fig. 3). The number average molecular weights (M_n) and polydispersity indices (PDI) determined by SEC were found to be 5.9 kDa and 1.05 for **6**, 7.9 kDa and 1.04 for **7**, 3.0 kDa and 1.08 for **8**, and 5.2 kDa and 1.05 for **9**. The SEC traces of cross-linked **8** and **9** showed monomodal distributions and significant shifts to low molecular weights without traces of intermolecularly cross-linked high molecular weight species (Fig. 3). The large reduction in mass by SEC relative to the theoretical change, which has been observed in previously reported cross-linked dendrimers,[16,17] indicates a significant reduction in the size of cross-linked PGD-PDIs **8** and **9**.

Subsequently, dihydroxylation of **8** and **9** was performed using 2 mol% of $K_2OsO_4 \cdot 2H_2O$ per alkene and conversions to cross-linked PGD-PDIs **3** and **4**, respectively, were verified by ^{1}H NMR spectra showing complete disappearance of the alkene peaks at δ 6.0-5.4 ppm. In the MALDI spectra of **3** and **4**, the most intense peak was observed at 4731.7 *m*/*z* for **3** and 8360.3 *m*/*z* for **4** that correspond to the complete addition of 32 and 64 hydroxyl groups, respectively (Fig. 2). The successful dihydroxylation suggests that the alkene groups in **8** and **9** are located at their surface or the cross-linked, polyallylated PGD-PDIs are sufficiently flexible for the catalyst to access each alkene group.

The evaluation of **3** and **4** by SEC in water was not possible because both aggregated in aqueous medium at concentrations of $>10^{-4}$ M, leading to extremely broad peaks. Thus, it is assumed that the size contraction upon RCM-mediated cross-linking observed for **8** and **9** in DMF is also observed in water for **3** and **4**. Some support for this assumption comes from the comparison of M_n values determined by SEC in DMF where M_n = 8.5 kD for **1** and M_n = 6.4 kD for **3**. Furthermore, previous work has shown analogous cross-linked dendrimers to be quite rigid and not exhibiting significantly different sizes with changes in solvent.[17] A direct comparison of **2** and **4** by SEC could not be made because **2** was not sufficiently soluble in DMF.

All of the synthesized PGD-PDIs **1**–**4** are water-soluble and display absorption and emission maxima in water at 567–572 nm and 606–612 nm, respectively, consistent with those of the

nondendronized PDI analogues reported in the literature (Fig. 4).[6] The fluorescence quantum yields measured in water ranged from 0.30 to 0.83, and the large difference can be attributed to the varying degrees of encapsulation and solubilization of PDIs within the polyglycerol dendritic shell. Thus, the attachment of four polyglycerol dendrons in **1** resulted in a quantum yield of 0.62, which is comparable to 0.58 of the ionic, nondendronized PDI **5** wherein four aryl sulfonate groups in the bay region are sufficient to provide water-solubility. This result suggests that 64 hydroxyl end-groups on the four dendrons are sufficient to allow these uncharged PDIs to exhibit excellent water-solubility and fluorescence in water.

The bulkier and more site-isolated PGD-PDI **2** exhibited an increased quantum yield of 0.83, which suggests a more effective encapsulation and solubilization of the PDI fluorophore by mostly eight dendrons carrying a total of 128 peripheral hydroxyl groups. Lastly, the quantum yields of cross-linked PGD-PDIs were determined to be 0.30 for **3** and 0.61 for **4**, lower in comparison to their uncross-linked structures **1** and **2**, respectively. There are several possible explanations for the tighter shell leading to a lower quantum yield. One is that **3** and **4** possess only half as many hydroxyl end-groups as the uncross-linked **1** and **2**, respectively, suggesting that the reduced polarity or lower aqueous solubility might correlate with a decrease in quantum yield. This idea is supported by the similar quantum yields observed for **1** and **4**, in which hydroxyl groups are present in approximately equal amounts. Also, the imide-substituted polyglycerol PDIs reported by Haag[7] (*vide infra*) showed a generation-dependent quantum yield, which was attributed to a reduction in aggregation with the larger more hydrophilic shells.

To probe further the protective effect of polyglycerol dendrons on PDIs, the fluorescence response (F/F_0) of PGD-PDIs **1**–**4** was monitored in the presence of a variety of metal ions as fluorescence quenchers and compared to that of nondendronized PDI **5** under the same conditions (Fig. 5). Upon the addition of 100 equivalents of each metal ion, **5** showed significant fluorescence quenching with several metal ions (*e.g.*, F/F_0 = 0% for Cu^{2+}, 9% for Fe^{3+}, 35% for Pb^{2+}, 57% for Co^{2+}, and 64% for Ni^{2+}), whereas **1**–**4** remained fluorescent in all cases, indicating that the fluorescent PDI cores are indeed protected by the polyglycerol dendrons in water. Although PGD-PDIs were nearly insensitive to metal ions, slight differences in the extent of fluorescence quenching were observed (*e.g.*, F/F_0 > 95% for **2**, > 90% for **1** and **4**, and > 80% for **3** in most cases). The F/F_0 ratio increases in the order, **2** > **1** ~ **4** > **3**, which correlates with the size of the PGD-PDIs. This relative insensitivity of the PGD-PDIs to quenching means that further chemical modifications that may require the use of metals to incorporate new functional groups for bioconjugation can be performed without concern for residual metal ion quenching.

In our initial report, we showed that the attachment of four polyglycerol dendrons to the bay region of PDIs, afforded complete solubility in water without altering the fluorophore photostability. Thus, biotinylated analogues of PGD-PDI **1** and PDI **5** exhibited almost identical photostabilities.[9] In this study, we further investigated the effect of varying degrees of encapsulation on the photostability by monitoring the fluorescence intensity of PGD-PDI **1** in comparison to **2**–**4** upon 532 nm laser excitation. Figure 6 shows the photobleaching decay as a function of time, and in all cases the decay was fit reasonably well to a single exponential in which the fitted lifetime was defined as the photobleaching time: $\tau_{photobleaching}$ = 147 ± 7 s for **1**, 152 ± 6 s for **2**, 221 ± 8 s for **3**, and 268 ± 8 s for **4** ($\ln(2) \times \tau_{photobleaching} = t_{1/2}$). However, the decomposition processes were clearly more complex because log plots showed significant curvature.

In comparing the relative stabilities, there were no dramatic differences between **1**–**4**, but clear trends were seen by comparing the fluorescence at various time points. For example,

after 20 min irradiation, the remaining fluorescence ($F/F_0 \times 100\%$) was only 8% of the orignial value for **1** and 12% for **2**, whereas the cross-linked **3** and **4** retained more of their original intensity at 22% and 28%, respectively. This result indicates that the intramolecular cross-linking significantly enhances the photostability, most likely as a result of a tighter and more protective dendritic shell around the PDI chromophore, whereas the progression from four to eight dendrons provides minimal additional photostability.

3. Conclusions

We have developed straightforward methodology for solubilizing and protecting hydrophobic dyes in aqueous media by attaching water-soluble polyglycerol dendrons to the dye cores, including intramolecular cross-linking of the dendritic shells using the RCM reaction. Water-insoluble perylenediimides were used as the dye core and the resulting PGD-PDIs were water-soluble and fluorescent as a result of reduced aggregation in water. A key advance was the ability of uncharged, site-isolated PGD-PDIs to retain their fluorescence signals in the presence of a variety of metal ions as fluorescence quenchers, in contrast to the ionic nondendronized PDI analogue displaying significant fluorescence quenching over some metal ions. Further, RCM-based cross-linking provided a significant reduction in the size of PGD-PDIs while providing additional photostability. Thus, an important design principle emerges that suggests a smaller, tighter dendritic shell can outperform a larger, uncross-linked one. The overall approach based on the dendritic encapsulation clearly improves dye properties and allows for preparation of highly stable and biocompatible fluorophores that may be useful in a broad range of biological applications.

4. Experimental

General Methods

All reagents were purchased from Acros Organics, Alfa Aesar, AK Scientific, or Sigma-Aldrich, and used without further purification unless otherwise noted. NMR spectra were recorded using a Varian Unity 400 or 500 MHz spectrometer. Chemical shifts are reported in ppm and referenced to the corresponding residual proton in deuterated solvents. Mass spectral analyses were provided by the Mass Spectrometry Laboratory, School of Chemical Sciences, University of Illinois, using MALDI-TOF on an Applied Biosystems Voyager-DE STR spectrometer. GPC analyses were carried out using a Viscotek Model 300 TDA with DMF as the eluent and a flow rate of 1 mL/min on a series of three Viscogel columns. All GPCs were calibrated using poly(styrene) standards and carried out at 25 °C. M_w, M_n, and PDI represent the weight-average molecular weight, number-average molecular weight, and polydispersity index, respectively. UV-Vis absorbance spectra were recorded on a Shimadzu UV-2501PC spectrophotometer. Fluorescence spectra were recorded on a Horiba Jobin Yvon Fluoromax-3 spectrophotometer and quantum yields were determined using cresyl violet ($\Phi = 0.54$ in MeOH) as a reference. Photobleaching experiments were performed using a 532 nm Nd:YAG laser (Brimrose), in which 1 μL of PGD-PDI solution (0.1 μM) was placed on a microscope slide, covered with a glass coverslip, and excited with the laser power set at 20 mW. The fluorescence was collected for 20 min with an exposure time of 1 s for 120 frames. Dialysis was performed using dialysis tubing (Sigma-Aldrich MWCO 1200 or Spectra-Por MWCO 3500) against water at 25 °C. PGD-PDIs **1**, **2**, **6**, and **7** [9], and PDI **5** [6c] were synthesized according to the previously published procedures.

General Procedure for RCM-Mediated Cross-Linking Reactions

To a solution of the desired amount of PGD-PDI **6** or **7**in anhydrous, degassed CH_2Cl_2 (300 mL) was added Grubbs' 2nd generation catalyst (4 mol% per alkene). The mixture was

stirred at 25 °C for 15 h under a nitrogen atmosphere, and ethyl vinyl ether (10 mL) was added and stirred at 25 °C for 2 h. Excess Si-DMT (a ruthenium scavenger) was added and the solution was stirred at 25 °C for 24 h. The mixture was filtered to remove the ruthenium scavenger and the filtrate was evaporated under reduced pressure to afford the crude PGD-PDI **8** or **9** that was further purified by column chromatography on silica gel using dichloromethane/methanol (20:1) as eluent.

PGD-PDI 8—PGD-PDI **8** (43 mg, 96%) was obtained from PGD-PDI **6** (50 mg, 11 μmol). ^{1}H NMR (400 MHz, $CDCl_3$, δ): 8.52-6.78 (br, 30H), 5.98-5.42 (br, 32H), 4.39-2.52 (br, 208H), 1.32-0.98 (br, 24H). MALDI (*m*/*z*): $[M]^+$ calcd for $C_{224}H_{294}N_6O_{68}$, 4156.0; found, 4179.1 $[M+Na]^+$. GPC: M_w = 3.2 kDa, M_n = 3.0 kDa, and PDI = 1.08.

PGD-PDI 9—PGD-PDI **9** (25 mg, 96%) was obtained from PGD-PDI **7** (30 mg, 3.7 μmol). ^{1}H NMR (400 MHz, $CDCl_3$, δ): 8.50-7.02 (br, 30H), 6.02-5.40 (br, 64H), 4.40-2.52 (br, 412H), 1.36-0.97 (br, 24H). MALDI (*m*/*z*): $[M]^+$ calcd for $C_{376}H_{530}N_{10}O_{128}$, 7233.5; found, 7251.6 $[M+Na]^+$. GPC: M_w = 5.4 kDa, M_n = 5.2 kDa, and PDI = 1.05.

General Procedure for Dihydroxylation

The desired amount of PGD-PDI **8** or **9**, K_2OsO_4•$2H_2O$ (catalytic amount), *N*-methylmorpholine-*N*-oxide (4 equiv. per alkene), and citric acid (1 equiv. per alkene) were dissolved in acetone/water/*tert*-butanol (5:5:1) and stirred at 25 °C for 15 h. Excess Smopex-105 (an osmium scavenger) was added and the solution was stirred at 25 °C for 24 h. The mixture was filtered to remove the osmium scavenger and the filtrate was evaporated under reduced pressure to afford the crude PGD-PDI **3** or **4** that was further purified by dialysis against water at 25 °C for 2 d.

PGD-PDI 3—PGD-PDI **3** (17 mg, 83%) was obtained from PGD-PDI **8** (18 mg, 4.3 μmol). ^{1}H NMR (400 MHz, CD_3OD, δ): 8.50-7.12 (br, 30H), 4.12-3.05 (br, 236H), 2.85-2.60 (br, 4H), 1.24-0.98 (br, 24H). MALDI (*m*/*z*): $[M]^+$ calcd for $C_{224}H_{326}N_6O_{100}$, 4700.0; found, 4731.7 $[M+Na]^+$. GPC: M_w = 6.9 kDa, M_n = 6.4 kDa, and PDI = 1.09. UV-Vis (H_2O):λ_{max} (ε) = 568 nm (23 650 $M^{-1}cm^{-1}$). Fluorescence (H_2O): λ_{max} (Φ) = 606 nm (0.30).

PGD-PDI 4—PGD-PDI **4** (25 mg, 91%) was obtained from PGD-PDI **9** (24 mg, 3.3 μmol). ^{1}H NMR (500 MHz, CD_3OD, δ): 8.46-7.10 (br, 30H), 4.20-3.12 (br, 472H), 2.86-2.64 (br, 4H), 1.28-1.03 (br, 24H). MALDI (*m*/*z*): $[M]^+$ calcd for $C_{376}H_{594}N_{10}O_{192}$, 8321.7; found, 8360.3 $[M+K]^+$. GPC: M_w = 9.9 kDa, M_n = 9.3 kDa, and PDI = 1.06. UV-Vis (H_2O): λ_{max} (ε) = 572 nm (28 850 $M^{-1}cm^{-1}$). Fluorescence (H_2O): λ_{max} (Φ) = 606 nm (0.61).

Acknowledgments

We gratefully acknowledge the National Institutes of Health (GM 87448) for financial support of this research.

References

1. a) Giepmans BNG, Adams SR, Ellisman MH, Tsien RY. Science. 2006; 312:217. [PubMed: 16614209] b) Schwartz JJ, Quake SR. Proc Natl Acad Sci USA. 2009; 106:20294. [PubMed: 19906998] c) Johnsson N, Johnsson K. ACS Chem Biol. 2007; 2:31. [PubMed: 17243781] d) Li GW, Xie XS. Nature. 2011; 475:308. [PubMed: 21776076] e) Rosi NL, Giljohann DA, Thaxton CS, Lytton-Jean AKR, Han MS, Mirkin CA. Science. 2006; 312:1027. [PubMed: 16709779]

2. a) Aubin JE. J Histochem Cytochem. 1979; 27:36. [PubMed: 220325] b) Ballou B, Ernst LA, Waggoner AS. Curr Med Chem. 2005; 12:795. [PubMed: 15853712] c) Kobayashi H, Ogawa M, Alford R, Choyke PL, Urano Y. Chem Rev. 2010; 110:2620. [PubMed: 20000749]
3. Lavis LD, Raines RT. ACS Chem Biol. 2008; 3:142. [PubMed: 18355003]
4. a) Langhals H. Chimia. 1994; 48:503.b) Pasaogullari N, Icil H, Demuth M. Dyes Pigments. 2006; 69:118.c) Weil T, Vosch T, Hofkens J, Peneva K, Müllen K. Angew Chem Int Ed. 2010; 49:9068.
5. a) Langhals H. Heterocycles. 1995; 40:477.b) Nagao Y. Prog Org Coatings. 1997; 31:43.c) Würthner F. Chem Commun. 2004:1564.d) Langhals H. Helv Chim Acta. 2005; 88:1309.e) Würthner F. Pure Appl Chem. 2006; 78:2341.f) Micheli E, D'Ambrosio D, Franceschin M, Savino M. Mini-Rev Med Chem. 2009; 9:1622. [PubMed: 20088777] g) Avlasevich Y, Li C, Müllen K. J Mater Chem. 2010; 20:3814.h) Huang C, Barlow S, Marder SR. J Org Chem. 2011; 76:2386. [PubMed: 21410184]
6. a) Margineanu A, Hofkens J, Cotlet M, Habuchi S, Stefan A, Qu J, Kohl C, Müllen K, Vercammen J, Engelborghs Y, Gensch T, De Schryver FC. J Phys Chem B. 2004; 108:12242.b) Qu J, Kohl C, Pottek M, Müllen K. Angew Chem Int Ed. 2004; 43:1528.c) Kohl C, Weil T, Qu J, Müllen K. Chem Eur J. 2004; 10:5297. [PubMed: 15382203] d) Jung C, Müller BK, Lamb DC, Nolde F, Müllen K, Bräuchle C. J Am Chem Soc. 2006; 128:5283. [PubMed: 16608365]
7. Heek T, Fasting C, Rest C, Zhang X, Würthner F, Haag R. Chem Commun. 2010; 46:1884.
8. a) Abdalla MA, Bayer J, Rädler JO, Müllen K. Angew Chem Int Ed. 2004; 43:3967.b) Peneva K, Mihov G, Nolde F, Rocha S, Hotta J, Braeckmans K, Hofkens J, Uji-i H, Herrmann A, Müllen K. Angew Chem Int Ed. 2008; 47:3372.c) Peneva K, Mihov G, Herrmann A, Zarrabi N, Börsch M, Duncan TM, Müllen K. J Am Chem Soc. 2008; 130:5398. [PubMed: 18376823] d) Yin M, Shen J, Pflugfelder GO, Müllen K. J Am Chem Soc. 2008; 130:7806. [PubMed: 18512911] e) Yin M, Shen J, Gropeanu RA, Pflugfelder GO, Weil T, Müllen K. Small. 2008; 4:894. [PubMed: 18561214] f) Cordes T, Vogelsang J, Anaya M, Spagnuolo C, Gietl A, Summerer W, Herrmann A, Müllen K, Tinnefeld P. J Am Chem Soc. 2010; 132:2404. [PubMed: 20121094]
9. Yang SK, Shi X, Park S, Doganay S, Ha T, Zimmerman SC. J Am Chem Soc. 2011; 133:9964. [PubMed: 21671621]
10. a) Grubbs RH, Miller SJ, Fu GC. Acc Chem Res. 1995; 28:446.b) Trnka TM, Grubbs RH. Acc Chem Res. 2001; 34:18. [PubMed: 11170353]
11. a) Calderón M, Quadir MA, Sharma SK, Haag R. Adv Mater. 2010; 22:190. [PubMed: 20217684] b) Haag R, Sunder A, Stumbé JF. J Am Chem Soc. 2000; 122:2954.
12. a) Kainthan RK, Janzen J, Levin E, Devine DV, Brooks DE. Biomacromolecules. 2006; 7:703. [PubMed: 16529404] b) Kainthan RK, Hester SR, Levin E, Devine DV, Brooks DE. Biomaterials. 2007; 28:4581. [PubMed: 17688941] c) Kainthan RK, Brooks DE. Biomaterials. 2007; 28:4779. [PubMed: 17706767] d) Wyszogrodzka M, Haag R. Biomacromolecules. 2009; 10:1043. [PubMed: 19351158]
13. a) Wyszogrodzka M, Möws K, Kamlage S, Wodzińska J, Plietker B, Haag R. Eur J Org Chem. 2008:53.b) Wyszogrodzka M, Haag R. Poly Mat Sci Eng. 2007; 48:760.c) Elmer SL, Man S, Zimmerman SC. Eur J Org Chem. 2008:3845.
14. Wilms D, Stiriba SE, Frey H. Acc Chem Res. 2010; 43:129. [PubMed: 19785402]
15. a) Sunder A, Mülhaupt R, Haag R, Frey H. Macromolecules. 2000; 33:253.b) Yeh PYJ, Kainthan RK, Zou Y, Chiao M, Kizhakkedathu JN. Langmuir. 2008; 24:4907. [PubMed: 18361531] c) Burakowska E, Haag R. Macromolecules. 2009; 42:5545.d) Zill A, Rutz AL, Kohman RE, Alkilany AM, Murphy CJ, Kong H, Zimmerman SC. Chem Commun. 2011; 47:1279.
16. a) Wendland MS, Zimmerman SC. J Am Chem Soc. 1999; 121:1389.b) Schultz LG, Zhao Y, Zimmerman SC. Angew Chem Int Ed. 2001; 40:1962.c) Zimmerman SC, Wendland MS, Rakow NA, Zharov I, Suslick KS. Nature. 2002; 418:399. [PubMed: 12140553] d) Burakowska E, Quinn JR, Zimmerman SC, Haag R. J Am Chem Soc. 2009; 131:10574. [PubMed: 19722631] e) Zill AT, Licha K, Haag R, Zimmerman SC. New J Chem. 201210.1039/c1nj20476a
17. a) Beil JB, Lemcoff NG, Zimmerman SC. J Am Chem Soc. 2004; 126:13576. [PubMed: 15493889] b) Lemcoff NG, Spurlin TA, Gewirth AA, Zimmerman SC, Beil JB, Elmer SL, Vandeveer HG. J Am Chem Soc. 2004; 126:11420. [PubMed: 15366871] c) Zimmerman SC, Quinn JR, Burakowska E, Haag R. Angew Chem Int Ed. 2007; 46:8164.

18. Scholl M, Ding S, Lee CW, Grubbs RH. Org Lett. 1999; 1:953. [PubMed: 10823227]

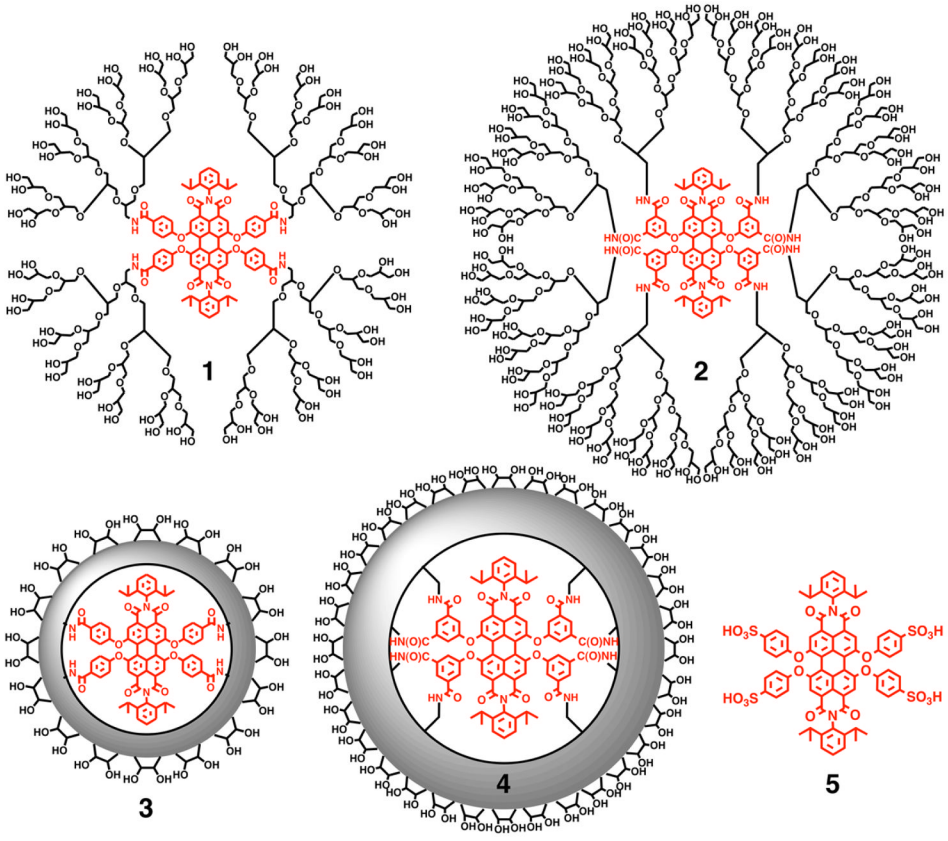

Figure 1.
Structures of PGD-PDIs **1**–**4** and PDI **5**.

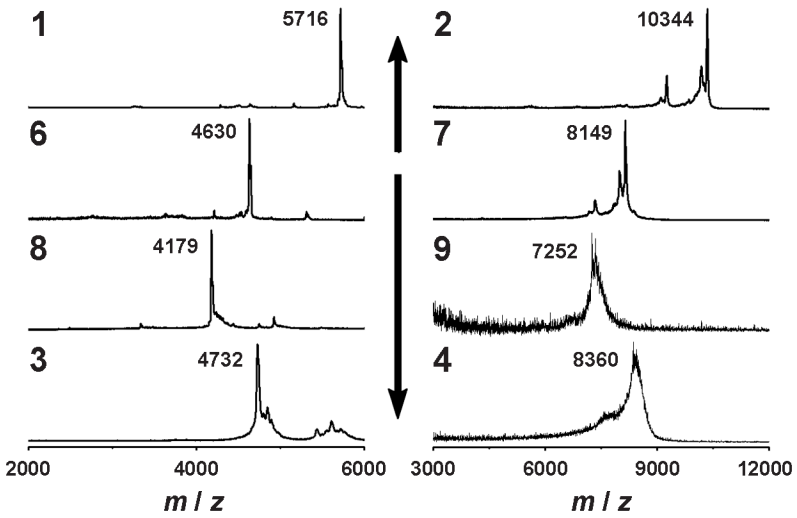

Figure 2.
MALDI-TOF mass spectra of PGD-PDIs **1**–**4** and **6**–**9**.

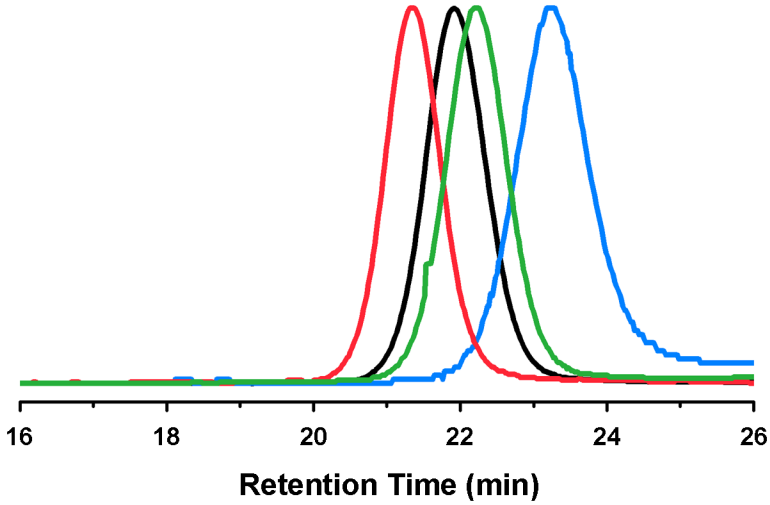

Figure 3.
SEC traces of PGD-PDIs **6** (black), **7** (red), **8** (blue), and **9** (green).

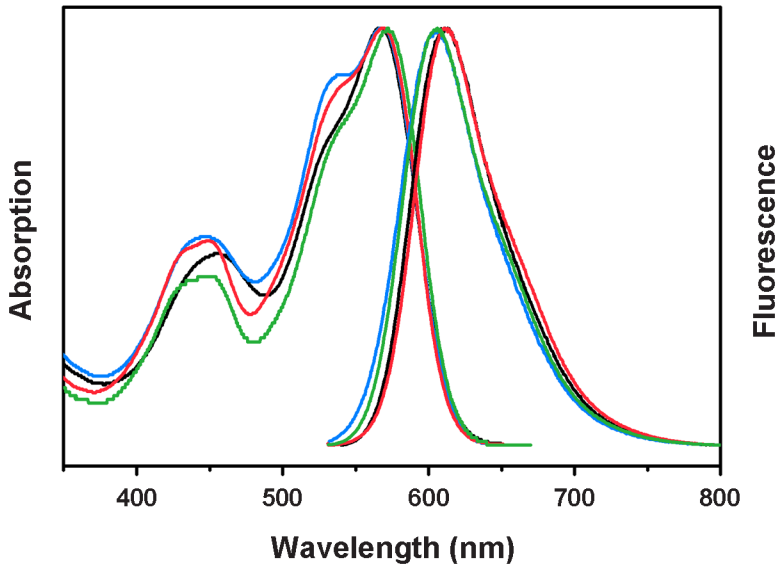

Figure 4.

Normalized absorption and fluorescence spectra of PGD-PDIs **1**–**4** in water. $\lambda_{abs,max}$ (nm), $\lambda_{flu,max}$ (nm), Φ (in water): 567, 612, 0.62 (**1**, black); 569, 612, 0.83 (**2**, red); 568, 606, 0.30 (**3**, blue); 572, 606, 0.61 (**4**, green).

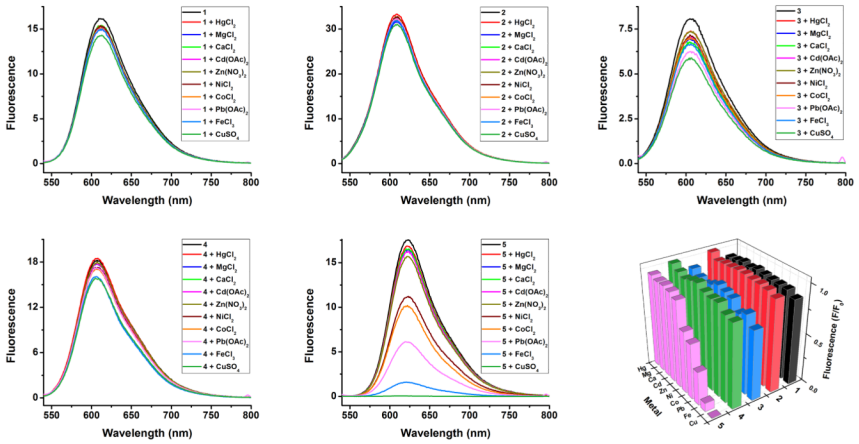

Figure 5.

Fluorescence spectra and response (F/F_0) of PGD-PDIs **1**–**4** and PDI **5** in water (1 μM) in the presence of metal ions (100 μM).

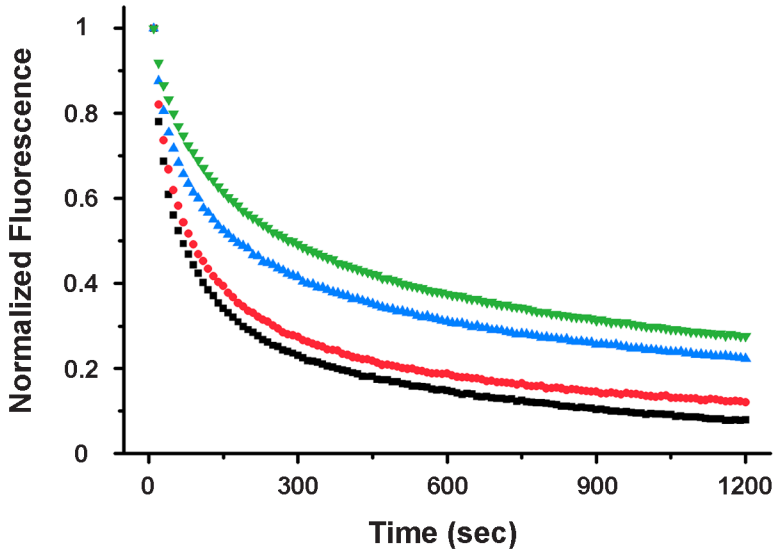

Figure 6.
Normalized fluorescence intensity of PGD-PDIs **1** (black), **2** (red), **3**, (blue), and **4** (green) as a function of time in water.

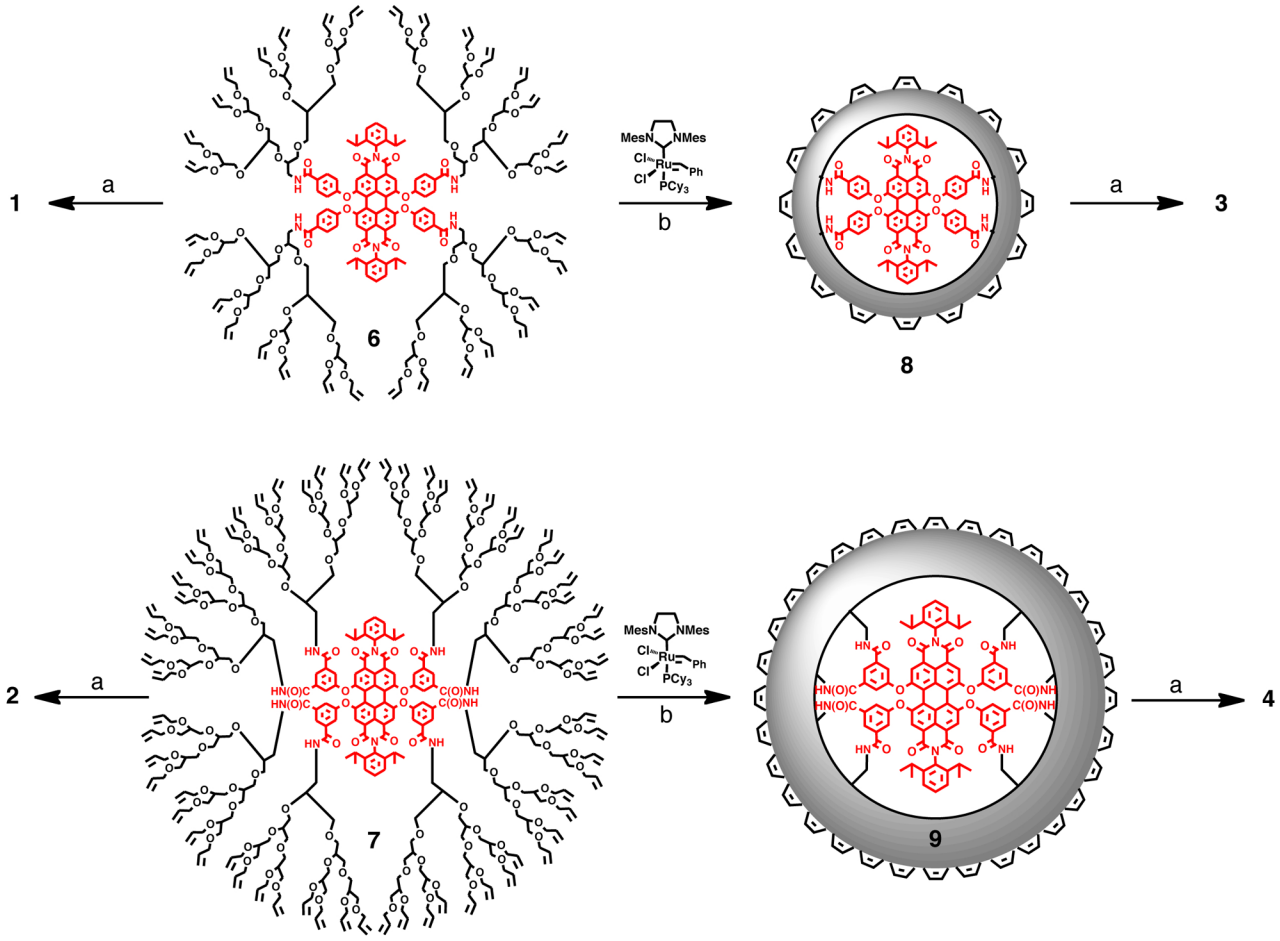

Scheme 1.

Synthesis of PGD-PDIs **1**–**4**. Reagents and conditions: (a) $K_2OsO_4 \cdot 2H_2O$, NMO, citric acid, acetone/*t*-BuOH/H_2O, 25 °C, 15 h; (b) CH_2Cl_2, 25 °C, 15 h.